JOURNAL OF MECHANICAL ENGINEERING AND SCIENCES
ISSN: 2289-4659 e-ISSN: 2231-8380
VOLUME 17, ISSUE 4, 2023, 9778 – 9790
DOI: https://doi.org/10.15282/jmes.17.4.2023.10.0774

UNIVERSITI MALAYSIA PAHANG AL-SULTAN ABDULLAH

RESEARCH ARTICLE

Optimization of offset and cant angle winglet on remote control airplane using Taguchi – Particle swarm optimization

B. Junipitoyo[1]*, S. Hariyadi S.P[1], F.D. Pertiwi[2], T.V. Kusumadewi[3], A. Rahmadi[4], and S.Z. Salsabila[3]

[1] Aircraft Maintenance Engineering, Politeknik Penerbangan Surabaya, 60236 Surabaya, Indonesia
Phone: +62318410871; Fax: +62318490005
[2] Department of Mechanical Engineering, Universitas Muhammadiyah Magelang, 56172 Magelang, Indonesia
[3] Mechanical Engineering Department, Faculty of Industrial Technology and Systems Engineering, Institut Teknologi Sepuluh Nopember Surabaya, 60111 Surabaya, Indonesia
[4] Mechanical Engineering Department, Universitas Muhammadiyah Pontianak, 78123 Pontianak, Indonesia

ABSTRACT - Incorporating winglets into aircraft has been empirically proven to notably improve aerodynamic efficiency by reducing vortex-induced effects at the wingtips. However, conducting comprehensive investigations necessitates the exploration of numerous winglet factors and value variations. This study pertains to remote control aircraft winglets, focusing on manipulating cant angle and offset factors across four distinct values. Two primary objectives guide this research: firstly, the maximization Cl/Cd_{max}, and secondly, the minimization Cd_0. The Taguchi experimental design is employed to randomize the variations in offset and cant angle values systematically. These variations are then used to generate pivotal regression values in the subsequent particle swarm optimization (PSO). The variance analysis evaluates the impact of winglet-related variables on each research goal. Additionally, the winglet design incorporates the open-source XFLR5 software, an accessible resource for aeromodelling clubs in Indonesia. XFLR5 enables the investigation of aerodynamic parameters across various angles of incidence and plays a crucial role in this research. The results of this study reveal that the Taguchi method yields two distinct combinations of factor values, aligning with the two primary research objectives. Conversely, particle swarm optimization generates a combination that effectively addresses both objectives. A comparative analysis of the winglet factor combinations from Taguchi and PSO underscores the greater efficiency of the PSO method in optimizing winglet variations for two distinct objectives.

ARTICLE HISTORY
Received : 08th Oct. 2022
Revised : 10th Oct. 2023
Accepted : 22nd Nov. 2023
Published : 26th Dec. 2023

KEYWORDS
Offset winglet
Cant angle
Remote control airplane
Taguchi
PSO

1.0 INTRODUCTION

Aeromodelling is an aircraft testing methodology employing remote control (RC) airplanes or gliders. In the Indonesian context, aeromodelling has undergone progressive evolution since 1946, encompassing multifaceted endeavors involving aeromodelling aircraft design, fabrication, and testing. The trajectory of aeromodelling advancement is intertwined with the emergence of uncrewed aerial vehicles (UAVs), commonly called unmanned aerial vehicles, which elicit a dedicated following driven by their pursuit of specific objectives. In an uncrewed vehicle, where the available onboard fuel solely constrains endurance, the maximization of flight duration essentially hinges upon configuration efficiency. Simultaneously, the adaptability and capacity of UAVs (fixed-wing) can be enhanced to a greater extent by improving performance metrics such as top speed, stall threshold, ascent rate, and maneuvering radius. Consequently, pursuing research endeavors and formulating specialized protocols, layouts, and methodologies aimed at weight reduction, aerodynamic optimization, and overall performance enhancement of fixed-wing UAVs represent pivotal strides within unmanned aviation [1]. In aerial dynamics, commercial aircraft, remote-controlled (RC), and unmanned aerial vehicle (UAV) aircraft experience congruent force profiles during flight. These forces encompass thrust, drag, lift, and weight, collectively influencing the aircraft's in-flight manipulation. Among these forces, lift and drag manifest as outcomes of a linear interplay between the aircraft and the surrounding air medium [2]. While lift constitutes a vector perpendicular to the prevailing wind direction, drag forces are a vector aligned with the wind flow [3]. The interrelation between these two forces engenders a resultant force vector acting upon the aircraft.

Extensive investigations have been conducted in aerodynamic forces, specifically drag and lift, encompassing strategies to mitigate vortex-induced phenomena within aircraft. Among these strategies, integrating winglets at the terminus of aircraft wings has emerged as a noteworthy approach. Numerous scholarly investigations have highlighted the utilization of winglets on both commercial airplanes and UAVs, showcasing their ability to significantly reduce drag and alleviate the formation of trailing vortices at wingtips [4–7]. An initial configuration about the choice of winglet characteristics can be embraced to achieve intermediate and elevated levels of precision. Various software tools, including XFOIL and XFLR5, can execute two-dimensional (2D) and three-dimensional (3D) evaluations of aerodynamic phenomena near wings and bodies. These tools further facilitate direct and inverse procedures for airfoil design within

*CORRESPONDING AUTHOR | B. Junipitoyo | ✉ ararya.pendopo@gmail.com

the two-dimensional context and enable holistic design considerations encompassing body structures, the center of gravity (CoG), moment of inertia assessments, and stability analyses within the three-dimensional framework [1]. Sethi and Ahlawat [8] contend that XFLR5 software is utilized to derive preliminary static stability parameter estimations, providing an informed basis for evaluating the aircraft's performance and stability characteristics. According to Adawy et al. [9], XFLR5 represents a computational tool intended to analyze individual airfoil elements. Along the same line, Kontogiannis et al. [10] emphasized the critical role of XFOIL and XFLR5 codes in refining grid selection for computational fluid dynamics (CFD), enhancing the precision of the three-dimensional models used in the detailed design phase.

Various geometries of winglet designs have been investigated in prior research to attain an optimal geometric configuration. These investigations encompass a spectrum of methodologies, ranging from numerical analysis to incorporating machine learning and metaheuristic techniques, to achieve the desired objectives. Whitcomb [6] explored the design of upper and lower winglets with wind tunnel method. The design parameters for the upper winglet encompass spanwise load distribution, height, planform, airfoil selection, angles of incidence and twist, as well as cant angle or dihedral. The outcomes revealed a correlation between the incremental enhancement in overall performance facilitated by winglets and the angles of incidence. Panagiotou et al. [4, 5, 11] employed computational fluid dynamics (CFD) in their numerical investigation to scrutinize alterations in winglet configuration geometry. The study encompassed a comprehensive assessment of diverse parameters, including height, blending radius, winglet airfoil profile, taper ratio, and cant angle, to discern their respective impacts on the lift-to-drag ratio and stall characteristics. Moreover, Guerrero et al. [12] illustrated incorporating cant angle and sweep angle within winglet design using CFD software for analysis. The winglet geometry exerts a discernible influence on enhancing aerodynamic performance across various angles of attack.

Based on prior studies, many geometric configurations for winglet design have been selected to pursue specific objectives. Moreover, the objectives typically encompass a multi-objective approach rather than being solely directed toward a single objective. The selection of an appropriate configuration aligned with the intended objectives necessitates the application of meticulous methodologies. Among these methodologies, one prevalent approach involves utilizing optimization techniques, such as the Taguchi method, rooted in statistical principles or metaheuristic algorithms founded upon artificial intelligence principles. The methodology employed for implementing optimization techniques involves constraining the design domain, investigating discrete subsets encompassing the various factors and levels of interest, and ensuring the preservation of data precision devoid of extraneous disturbances. This confluence can be achieved by employing Experimental Design (DOE), a technique rooted in statistical science, to forge an efficacious design domain ahead of the empirical inquiry. The term "experiment" denotes various forms of optimization undertaken experimentally or computationally within real-world conditions. The utilization of DOE has been extensively embraced in aeronautical studies, exemplified by endeavors such as optimizing multidisciplinary aircraft wing design [13].

Using the Taguchi experimental design, Kapsalis et al. [13] explored the Blended-Wing-Body (BWB) configuration using CFD. Using Taguchi methods resulted in a significant reduction of approximately 70% in the requisite number of computational analyses compared to a comprehensive full factorial approach. This outcome underscores the potential to uphold the accuracy of computational modeling while concurrently achieving substantial resource economization. Atencio et al. [14] employed Taguchi's orthogonal arrays to discern a diminished set of experiments for ascertaining optimal UAV flight parameter values while upholding the statistical robustness of experimental outcomes. Using Taguchi's arrays, the total number of requisite experiments to ascertain optimal flight parameters (a sum of 25) was substantially curtailed when juxtaposed with alternative experiment design methodologies.

The application of multidisciplinary optimization to RC plane wing design has demonstrated successful outcomes through integrating experimental design and hybrid machine learning - metaheuristic techniques, as evidenced by several investigations [15–18]. This paradigm has served as a benchmark for scrutinizing alternative algorithms within aviation. Notably, Particle Swarm Optimization (PSO) is an exemplar among optimization approaches, deriving inspiration from natural behaviors and characterized by its simplicity and comprehensibility. Particle Swarm Optimization (PSO) harnesses the communal patterns seen in animal groups, similar to the coordinated movements of fish schools or bird flocks. PSO algorithm is founded upon the emulation of these group behaviors. Its notable advantages encompass rapid convergence, a proficient exploration mechanism, reduced reliance on initial conditions, computational simplicity, and ease of implementation. Abnous et al. [19] explored PSO to design a blended wing body for developing the feasibility or performance of blended wing body-Integrated Transitioning UAV. The results state that PSO can achieve the higher performance than baseline designs. PSO can be applied in airfoil design for UAVs [20–23], and PSO proved that this method can solve the aerodynamics role model for UAVs. PSO also can solve dynamic stability for UAVs. As same as Abnous et al, Bashir et al [24] investigated aerodynamic and performance camber adaptive winglet with PSO; this study explores the utilization of optimization methodologies. It juxtaposes diverse winglet configurations, elucidating that modifying winglet geometries during flight operations can yield improvements in aircraft performance by mitigating aerodynamic drag and reducing fuel consumption. Tao et al. [25] utilized PSO to optimize wing configurations at critical drag divergence Mach Numbers. Their study results demonstrate a dual impact of PSO: it not only significantly reduces drag coefficients for both the airfoil and wing during cruise Mach numbers but also efficiently mitigates the increase in drag as the Mach number rises, extending up to the drag divergence Mach Number threshold. The literature review reveals that PSO proves advantageous in optimizing aircraft design, including its utility for optimizing winglet design [24, 26–28].

Traditionally, RC aircraft design, notably winglet design, has relied on a trial-and-error approach. Furthermore, optimal results with reduced stochasticity can be achieved by judicious choice of suitable parameters. This manuscript introduces a straightforward and effective metaheuristic algorithm, PSO, to mitigate these challenges. This approach is specifically tailored for scenarios characterized by minimal computational demands, thereby rendering it suitable for the computation of aerodynamic coefficients. Adopting this technique offers valuable support to the aeromodelling community engaged in RC airplane design by providing a cost-effective means for advancing their design endeavors.

In this contemporary investigation, Taguchi's experimental design methodology and variance analysis (ANOVA) were employed to construct a regression equation, which was utilized to identify optimal PSO parameters within the context of winglet design optimization. The discretized offset winglet and cant angle values were subjected to PSO-optimized parameters. The utilization of PSO is employed to address multi-objective challenges that lie beyond the capabilities of the Taguchi method.

2.0 METHODS AND MATERIALS

This study uses four steps in the optimization design. These methods are the determination of the DOE of the winglet factor and retrieving response data with XFLR5, processing response data with Taguchi, determining the objective function for optimization, and optimizing PSO using predetermined parameters.

2.1 Winglet Geometry Design with XFLR5

This study uses a fixed-wing RC aircraft with an airfoil Cal2263m [29], root chord wing of 189 mm, tip chord wing of 136 mm, and span of 518 mm [30]. The winglet geometry under review (Figure 1) is winglet offset and cant angle with winglet chord tip measuring 0.21Ct (tip chord) [6] and winglet height 0.5Ct (tip chord). Cant angle was simulated by incorporating a minor curvature radius at the junction between the winglet and the wingtip, ensuring a seamless transition between the two components. Furthermore, an examination was conducted to assess the impact of the winglet's offset on the wing's aerodynamic performance. Geometry design uses XFLR5 assistance by choosing winglet factors in the form of offset and cant angle because XFLR5 has limitations in making winglet designs [31]. XFLR5 uses XFOIL data in two dimensions to calculate lift, drag, pitching moment, and pressure coefficient [32]. XFLR5 only analyzes the wings, not the complete fuselage or tail of the aircraft, so that it tends to be faster and cheaper, and the purpose of making aircraft design is effective [33].

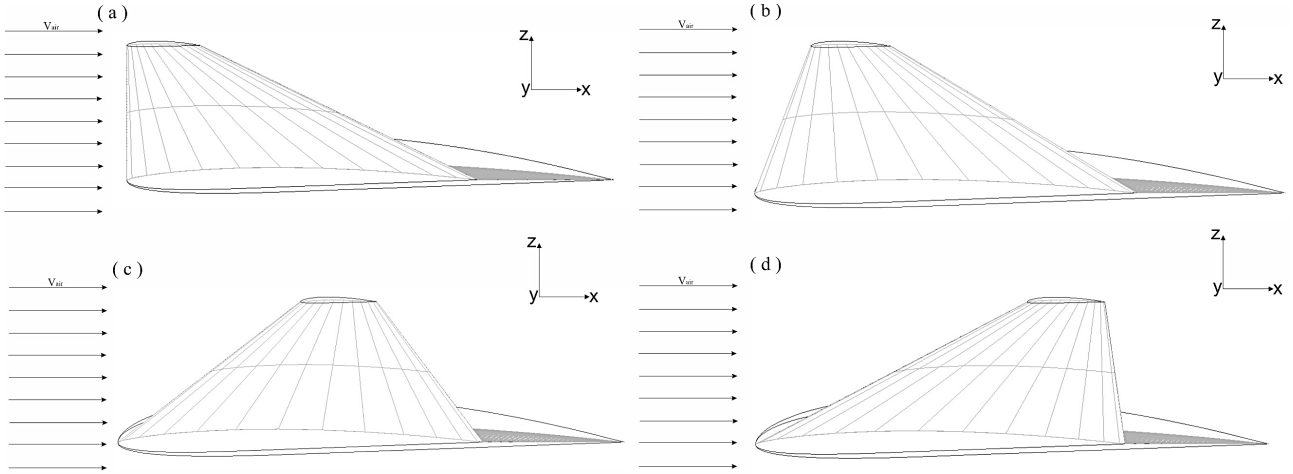

Figure 1. Variation of winglet offset with cant angle 50°: (a) offset 0 mm, (b) offset 50 mm, (c) offset 68 mm, and (d) offset 100 mm

XFLR5 analysis in this study uses polar type 2 (fixed lift) with ring vortex analysis (VLM2), the number of panels is 3519, the angle of incidence is -2° to 8° (increment 2°), and the angle of incidence exceeds 8° in this problem cannot be calculated by XFLR5, because the VLM method is an inviscid method that is not able to predict stalls [34]. The observed output values are the drag force when the angle of attack is 0° (Cd_0) and the maximum lifting force (Cl_{max}).

2.2 Winglet Objective Function

XFLR5 simulation produces aerodynamic performance using the linear vortex lattice method (VLM). VLM is is an approach for modeling inviscid flow. It is highly suitable for various wing configurations, encompassing wings with sweep, low aspect ratios, high dihedral angles, and the incorporation of winglets. VLM works by modelling wing perturbations on some of the vortices to the plane [34]. Lifting force and lift coefficient according to Deperrois [34] is as follows:

$$F = \rho V \times \Gamma \tag{1}$$

In Eq. (1), F= force of lift, ρ= density of fluid, and v= velocity of fluid. While the lift coefficient is determined as follows:

$$C_L = \frac{1}{\rho S v^2} \sum_{panels} F_{wz} \tag{2}$$

In Eq. (2), F_{wz} is a projection in the vertical wind direction, and S is the number of panel areas, for example, the surface area of the wing design. In the meantime, calculating the drag force involves the summation of the induced drag coefficient and the drag coefficient when the angle of incidence is at zero degrees using Eqs. (3) and (4) [32], AR for aspect ratio, e is the Oswald number.

$$C_D = C_{D_0} + \frac{C_L^2}{\pi . AR . e} \tag{3}$$

$$C_{Di} = \frac{C_L^2}{\pi . AR . e} \tag{4}$$

From Eqs. (1)-(4), an aircraft's most crucial aerodynamic performance depends on the lift and drag force. Various geometries of aircraft, especially winglet design, are used to reach the optimum aircraft performance. In this case, the multi-objective of winglet design can solve with PSO algorithm, and the simple objective function can follow:

$$f(x) = minimize\ Cd_0 - maximize\ Cl/Cd_{max} \tag{5}$$

with the limitation of the winglet design geometry, namely

$$0\ mm \leq offset\ winglet \leq 100\ mm \tag{6}$$

$$50^o \leq cant\ angle \leq 90^o \tag{7}$$

The imposition of constraints on winglet geometry draws from the capabilities of XFLR5 in winglet design. A winglet offset of 0 mm denotes that, within the winglet design, no alteration applies to the value of the winglet offset; it is generated directly by the program itself (see Figure 2). Furthermore, the boundary employs integer values (Eqs. (6) and (7)) to facilitate a streamlined manufacturing process.

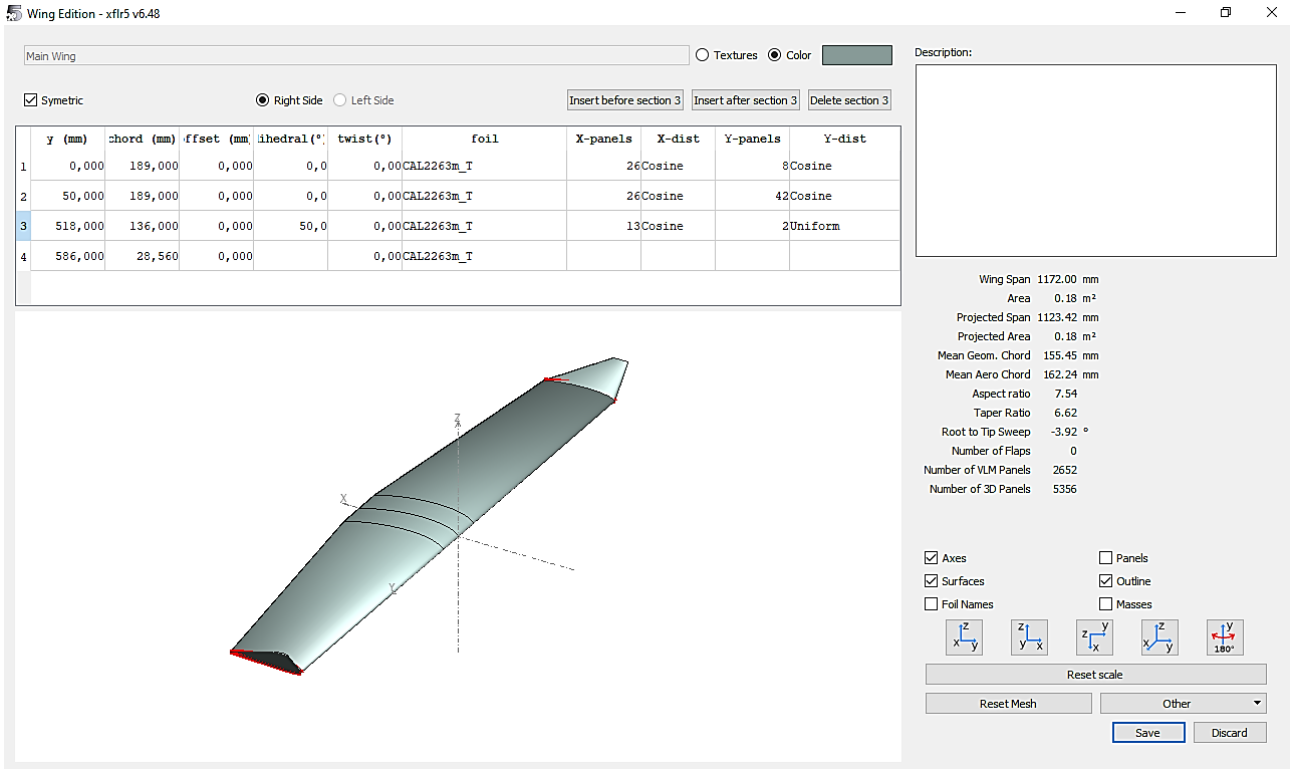

	y (mm)	chord (mm)	offset (mm)	dihedral(°)	twist(°)	foil	X-panels	X-dist	Y-panels	Y-dist
1	0,000	189,000	0,000	0,0	0,00	CAL2263m_T	26	Cosine	8	Cosine
2	50,000	189,000	0,000	0,0	0,00	CAL2263m_T	26	Cosine	42	Cosine
3	518,000	136,000	0,000	50,0	0,00	CAL2263m_T	13	Cosine	2	Uniform
4	586,000	28,560	0,000		0,00	CAL2263m_T				

Figure 2. Winglet offset (0 mm) in XFLR5

2.3 Taguchi Method

The Taguchi method improves product quality, time, and resources and minimizes costs. This method makes the product robust from the noise factor. The primary steps in this method are the planning stage, the implementation step, and the analysis step [35]. The experimental layout presented by Taguchi employs orthogonal arrays for structuring the process's influential parameters and varying levels. In contrast to the exhaustive assessment of all conceivable combinations, as seen in the full factorial design, the Taguchi method evaluates sets of combinations. This approach facilitates the acquisition of requisite data for ascertaining the foremost factors influencing product quality with a reduced

number of experimental runs. Consequently, this approach conserves time and resources while comprehensively understanding the factors' impact [36].

The preparatory phase of this investigation involves identifying levels for the winglet factor (Table 1) and selecting an appropriate orthogonal matrix. The decision regarding the orthogonal matrix stems from assessing the degrees of freedom associated with the winglet factor facilitated by the Minitab 16 software. Using Minitab 16, the $L_{16}(4^2)$ orthogonal array from Table 2 is chosen, signifying that the simulation experiment will be conducted 16 times without replication. Following the initial planning phase, the research progresses to the implementation stage, which involves the examination of factor combinations through experimentation using XFLR5. The experimental tests yield response variables, specifically Cl/Cd_{max} and Cd_0. Subsequently, the analysis phase is undertaken, where the Minitab 16 software is employed to calculate the amalgamation of factors and corresponding responses, culminating in the computation of the signal-to-noise (S/N) ratio. This ratio is pivotal in discerning the influence of both factors and their respective levels on the response variables. Notably, there exist three distinct categories of S/N ratios, each contingent upon the number of experimental repetitions, denoted as [35]:

i) Small is best

$$S/_N = -10log\left(\frac{1}{n}\sum_{i=1}^{r} Y_i^2\right) \tag{8}$$

ii) Nominal is best

$$S/_N = -10logV_e \tag{9}$$

$$S/_N = -10log\left(\frac{V_m - V_e}{nV_e}\right) \tag{10}$$

iii) Larger is best

$$S/_N = -10log\left(\frac{1}{n}\sum_{i=1}^{r} \frac{1}{Y_i^2}\right) \tag{11}$$

This study uses two types of S/N ratio, namely lower is better for Cd_0 response and bigger is better for Cl/Cd_{max} response. Furthermore, the method of variance analysis was employed to analyze the results, determine the performance qualifications for the optimal combination, and observe the effect of factors on the response [13].

Table 1. Factors and levels of the winglet

Factor	Level			
	1	2	3	4
Offset winglet (mm)	0	20	68	100
Cant angle (°)	50	60	70	90

Table 2. The number of simulations with orthogonal array $L_{16}(4^2)$

No	Factor	
	Offset winglet (mm)	Cant angle (°)
1	0	50
2	0	60
3	0	70
4	0	90
5	20	50
6	20	60
7	20	70
8	20	90
9	68	50
10	68	60
11	68	70

Table 2. (cont.)

No	Factor	
	Offset winglet (mm)	Cant angle (°)
12	68	90
13	100	50
14	100	60
15	100	70
16	100	90

2.4 Particle Swarm Optimization

Particle Swarm Optimization (PSO) represents an algorithm that works by imitating a flock of fish or a flock of birds. Reynolds experimented with the beauty of the choreography of flocks of birds in flight, while Hepner and Grenander studied the flocks to find ground rules regarding the probability of multiple birds gathering together, changing direction, and scattering [37]. Parsopoulos and Vrahatis [38] wrote that the early pioneers of this algorithm were social behaviour in observing flocks of birds, matching the velocity of the closest birds and acceleration based on the distance between birds was the primary basis in the flock foraging (Table 3). The mathematical model for PSO is based on a population of algorithms called swarms, while the individuals of the swarms are called particles. Swarm is determined by [38]:

$$S_w = \{x_1, x_2, \ldots., x_n\}, \tag{12}$$

n_p particles (selected individual candidates) are determined as:

$$x_i = (x_{i1}, x_{i2}, \ldots., x_{in})^T \in A_p, \quad i = 1, 2, \ldots., n_p \tag{13}$$

n_p is a predetermined algorithm tuning parameter. The objective function *f(x)* is calculated assuming it can apply to all particles in the member A_p thus ensuring that each particle possesses a distinct function value,

$$f_i = f(x)_i \in Y_p \tag{14}$$

The particles are assumed to be able to move along the search region, A_p. It allows an adjustment of the particle position, which is called the velocity and is shown as:

$$v_i = (v_{i1}, v_{i2}, \ldots., v_{in})^T \in A_p, \quad i = 1, 2, \ldots., n_p \tag{15}$$

Speed adjustments are executed using information from the preceding step, ensuring that each step conserves memory and yields the optimal position during the search process.

$$P = \{p_1, p_2, \ldots., p_n\}, \tag{16}$$

Consisting of,

$$p_i = (p_{i1}, p_{i2}, \ldots., p_{in})^T \in A, \quad i = 1, 2, \ldots., n_p \tag{17}$$

The position of the particles is determined:

$$p_i(t_p) = {}^{argmin}_{t_p} f_i(t_p) \tag{18}$$

$$p_g(t_p) = {}^{argmin}_{t_p} f(P_i(t_p)) \tag{19}$$

where, t_p is the number of iterations *and g* is the index of the best position with the smallest function value in *P*.

From Eqs. (12)-(19), the PSO equation is pioneered by Eberhart and Kennedy's formulas (1995) [38]:

$$v_{ij}(t_p + 1) = v_{ij}(t_p) + c_1 r_1 \left(p_{ij}(t_p) - x_{ij}(t_p)\right) + c_2 r_2 \left(p_{gj}(v) - x_{ij}(t_p)\right) \tag{20}$$

$$x_{ij}(t_p + 1) = x_{ij}(t_p) + v_{ij}(t_p + 1) \tag{21}$$

with i=1,2,….,n_p, j=1,2,…..,n_p. r_1 and r_2 are random numbers [0, 1], c_1 and c_2 are weighting factors, called the cognitive and social parameter.

Table 3. Pseudocode of PSO [38]

Input	Particles; swarm; best of position
1	**Begin** t: 0
2	**Initialize** the population of a swarm and best position
3	**Evaluate** swarm and best position and **set** global best of position index
4	**Whilst** (termination condition has yet to be satisfied)
5	**Restore** swarm Eqs.(20) and (21)
6	**Evaluate** swarm
7	**Update** best position redefines global best
8	**Set** t: t+1
9	**End Whilst**
10	**Print** best position found

Maurice Clerc [39]demonstrated the use of the constriction factor, k, which makes PSO more convergent. The constriction factor is written as:

$$V_{ij}(t_p+1) = kV_{ij}(t_p) + c_1R_1\left(p_g(t_p) - x_{ij}(t_p)\right) + c_2R_2\left(Gbest(t_p) - x_{ij}(t_p)\right)) \quad (22)$$

$$k = \frac{2}{\left|2 - \emptyset - \sqrt{\emptyset^2 - 4\emptyset}\right|} \quad (23)$$

$\emptyset$ is a function with components c_1 and c_2, $\emptyset = c_1 + c_2$, and $\emptyset > 4.0$. $\emptyset$ for good results is in the range of $4.1 < \emptyset < 4.2$ [39]. The inertia weight uses the following equation:

$$w_m = w_{min} + \frac{(w_{max} - w_{min})(t_{p_{max}} - t_p)}{t_{p_{max}}} \quad (24)$$

The inertial weight (w) is used as the PSO parameter because w is created to guard against particle search and exploitation. It is done because a small w is more easily trapped in the local optimum. The inertial weight that can make the particles find the global optimum is 0.8 to 1.2 [39]. While for c_1 and c_2 used in this study is 2.05, this value is based on research from Lee & Tuegeh (2020), which produces a good solution with the following velocity equation:

$$V_{ij}(t_p+1) = k(w_mV_{ij}(t_p) + c_1R_1\left(p_g(t_p) - x_{ij}(t_p)\right) + c_2R_2\left(Gbest(t_p) - x_{ij}(t_p)\right)) \quad (25)$$

3.0 RESULTS AND DISCUSSION

3.1 Taguchi for Aerodynamic Performance

The performance outcomes derived from the DOE, as presented in Table 1, were acquired through the utilization of the XFLR5 software. For each DOE configuration, data were meticulously collected at six distinct angles of attack, spanning from -2° to 8° with a consistent 2° increment. The ensuing results emanate from the judicious selection of the maximum Cl/Cd_{max} value, alongside the minimum Cd_0 value, from this comprehensive dataset. Subsequently, the response (aerodynamic performance) was reevaluated using the Taguchi robust parameter methodology. In the initial phase, Table 4 presents the computed results for Cl/Cd_{max} and Cd_0 responses, which Taguchi analyzed to derive the Signal-to-Noise (S/N) ratios. The S/N ratio for Cl/Cd_{max} is determined using Eq. (11), while the S/N ratio for Cd_0 is computed through Equation 8. Aerodynamic performance is assessed based on the *bigger is better* criterion for Cl/Cd_{max} and the *smaller is better* criterion for Cd_0.

Table 4. Aerodynamic performance results and S/N ratio

No	Response		S/N ratio	
	Cl/Cd_{max}	Cd_0	Cl/Cd_{max}	Cd_0
1	16.6273	0.01855	24.41643	34.63312
2	16.5415	0.01851	24.3715	34.65187
3	16.4495	0.01846	24.32305	34.67537
4	16.2625	0.01835	24.22375	34.72728
5	16.6242	0.01864	24.41482	34.59108
6	16.5375	0.01859	24.3694	34.61441
7	16.4436	0.01855	24.31994	34.63312
8	16.2464	0.01844	24.21514	34.68478

Table 4. (cont.)

No	Response		S/N ratio	
	Cl/Cd_{max}	Cd_0	Cl/Cd_{max}	Cd_0
9	16.6072	0.01879	24.40593	34.52146
10	16.519	0.01875	24.35968	34.53997
11	16.215	0.01871	24.30826	34.55852
12	16.2087	0.01862	24.19496	34.60041
13	16.624	0.01879	24.41471	34.52146
14	16.5358	0.01874	24.3685	34.54461
15	16.4368	0.0187	24.31635	34.56317
16	16.2197	0.0186	24.20086	34.60974

Tables 5 and 6 present the optimal levels and ranking based on the mean responses. Table 5 shows the influence of the cant angle on the Cl/Cd_{max} ratio and the best value (*) at level 1 for all factors. Notably, the cant angle has a more pronounced effect on Cl/Cd_{max}, contributing to enhanced lift performance without a concurrent increase in parasite drag. This phenomenon is ascribed to the ability of the cant angle to promote a more even pressure distribution across both the upper and lower surfaces of the wing, thus influencing aerodynamic performance. Additionally, the cant angle aids in the mitigation of trailing vortex formation at the wingtip, increasing the lift coefficient.

Table 5. Means of responses for Cl/Cd_{max}

Level	Offset	Cant Angle
1	16.47*	16.62*
2	16.46	16.53
3	16.44	16.44
4	16.45	16.23
Delta	0.03	0.39
Rank	2	1

* Best level

Table 6 reveals the influence of offset on Cd_0, with the optimal value ([a]) observed at level 3 and the optimal cant angle at level 1. Offset can mitigate parasite drag in RC airplanes by influencing airflow around the wing. Introducing an offset in a winglet can reduce frictional drag as it alters and redistributes the airflow patterns along the wing surface. This alteration diminishes frictional drag, a significant contributor to parasitic drag.

Table 6. Means of responses for Cd_0

Level	Offset	Cant Angle
1	0.01847	0.01869*
2	0.01855	0.01865
3	0.01872*	0.01861
4	0.01871	0.01850
Delta	0.00025	0.00019
Rank	1	2

* Best level

While considering Figures 3 and 4, we observe the S/N ratio plots corresponding to each response variable. In its traditional application, it is important to highlight that the Taguchi method is intended for optimizing individual responses rather than simultaneously optimizing multiple responses. Figure 3 depicts the optimal outcomes of Taguchi's approach for the *bigger is better* Cl/Cd_{max} criterion, which is associated with offset (level 1) and cant angle (level 1). In contrast, Figure 4 illustrates Taguchi's optimal results for the *smaller is better* Cd_0 criterion, where the optimal settings feature offset (level 3) and cant angle (level 1).

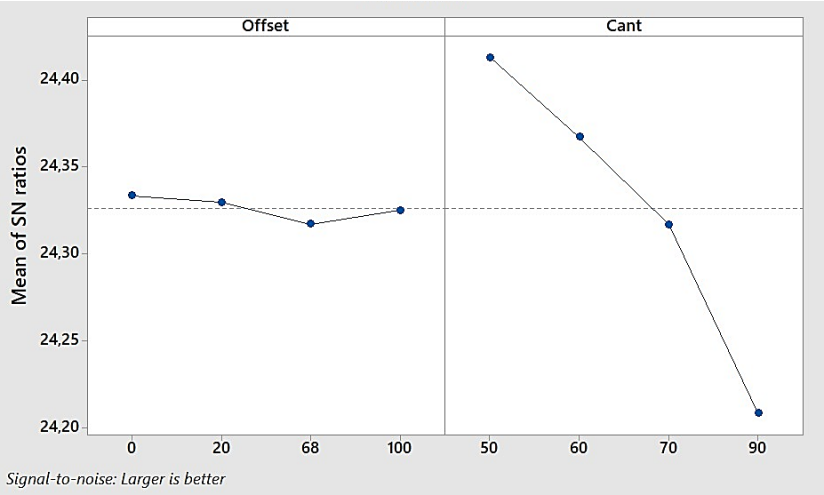

Figure 3. Graph of S/N ratio for Cl/Cd_{max}

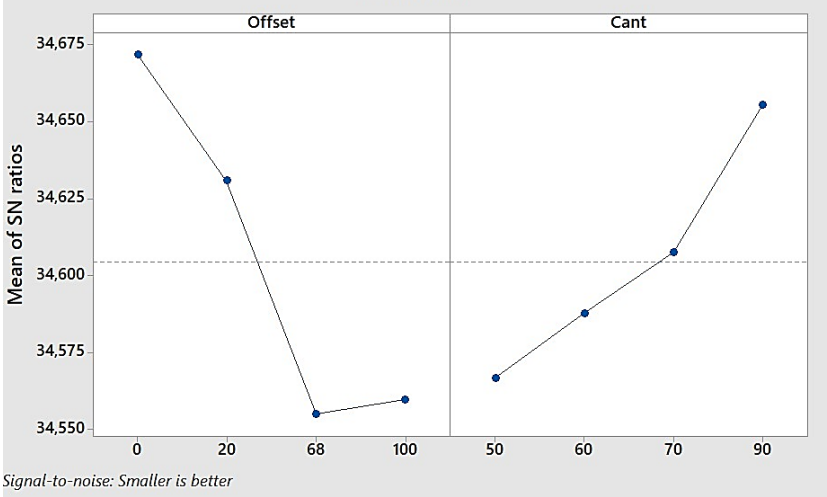

Figure 4. Graph of S/N ratio for Cd_0

The second stage involves conducting ANOVA calculations for each response variable. This stage is conducted to assess the influence of factors on individual responses. The results of the ANOVA for each response are presented in Table 7 - 8, and the significance of each factor's impact can be determined by examining the resulting P-values. A factor is considered influential when the P-value is less than 0.05. Table 7-8 reveals that the P-values obtained for both the Cl/Cd_{max} and Cd_0 responses are less than 0.05 for both factors. It can be concluded that the offset and cant angle factors significantly affect both responses.

Table 7. ANOVA results for Cl/Cd_{max}

Source	DF	Adj SS	Adj MS	F-Value	P-Value
Offset	3	0.002150	0.000717	10.06	0.003
Cant	3	0.330337	0.110112	1544.83	0.000
Error	9	0.000641	0.000071		
Total	15	0.333129			

Table 8. ANOVA results for Cd_0

Source	DF	Adj SS	Adj MS	F-Value	P-Value
Offset	3	0.000000	0.000000	1310.91	0.000
Cant	3	0.000000	0.000000	584.26	0.000
Error	9	0.000000	0.000000		
Total	15	0.000000			

Due to the limitations of the Taguchi method, this study incorporates an additional approach to calculate multiple responses to optimize the RC airplane's performance. PSO is employed as a complementary method to enhance the robustness of the Taguchi results. Taguchi's capabilities include generating a regression equation, the objective function for PSO optimization (as shown in Eqs. (26) and (27)). The objective function (Eq. (28)) for PSO can be subtitute Eqs. (26) and (27) in Eq.(5).

$$Cl/Cd_{max} = 17.1219 - 0.000212\ offset - 0.009709\ cant\ angle \tag{26}$$

$$Cd_0 = 0.018814 + 0.000003\ offset - 0.000005\ cant\ angle \tag{27}$$

$$f(x) = (0.018814 + 0.000003\ offset - 0.000005\ cant\ angle) - (17.1219 - 0.000212\ offset - 0.009709\ cant\ angle\ ) \tag{28}$$

3.2 PSO for Aerodynamic Performance

PSO simulation within this investigation is guided by a predefined set of parameters, including a swarm size of 1500, lower and upper bounds for inertia weight (w_{min}=0.8 and w_{max}=1.2), acceleration coefficients (c_1 and c_2), both set at 2.05, a constriction parameter (k) of 0.38 and a maximum iteration count of 100. The rationale for selecting w_{min} and w_{max} in order of 0.8 and 1.2, respectively, arises from inclination of particles to engage in global exploration, thereby achieving a balance between global and local exploration for optimal solutions [39]. The choice of c_1 and c_2 values as 2.05 is motivated by their efficacy in guiding the solution toward favorable outcomes [39]. The parameter values for swarm size and iteration count were determined through trial and error, leading to stability within these values. This study executed the PSO algorithm by iteratively testing various PSO parameters until a robust convergence was achieved. This convergence was monitored by evaluating the objective function values at each iteration (see Figure 5). The best fitness function value obtained from the PSO optimization results is -16.6179. Figure 5 also illustrates that the fitness function value converges steadily toward the target point from the 70th iteration onwards. The stability of this convergence pattern is attributed to the incorporation of inertia in the particle movement process. The convergence depicted in Figure 5 can also indicate that the PSO algorithm effectively addresses the scenarios considered in this study, ultimately leading to optimal values.

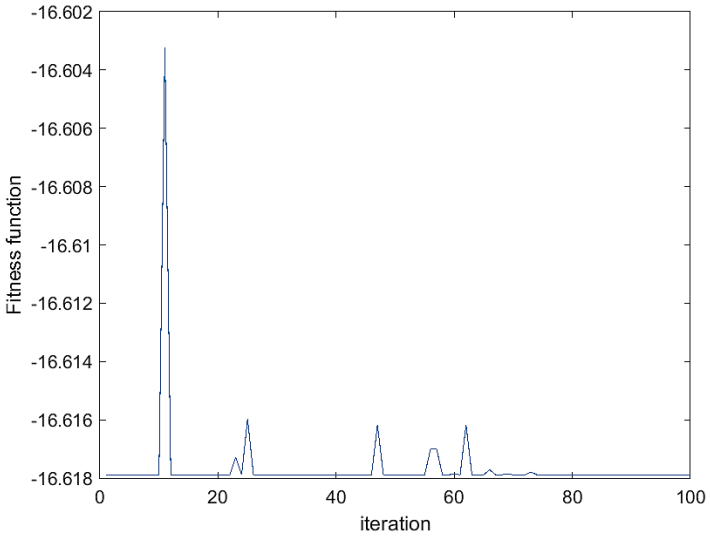

Figure 5. PSO fitness function

Furthermore, in addition to optimizing the fitness function, PSO generates factors identified as the top candidates in this study (Table 9). Notably, Table 9 reveals that these factors derived from the selected PSO results align with the order specified in the Design of Experiments (DOE) presented in Table 2. At the same time, the corresponding response values closely resemble those obtained from XFLR5 simulations.

Table 9. Comparison of XFLR5 and PSO results

	Factor		Response	
	Offset (mm)	Cant Angle (°)	Cl/Cd_{max}	Cd_0
XFLR5	0	50	16.6237	0.018554
PSO			16.63645	0.018564
Error (%)			0.0548	0.0538

The final step involves a comparison by substituting the results derived from PSO and Taguchi into Eqs. (26) and (27. This step is undertaken to assess which methods exhibit the capability to yield optimal values per the desired objectives. The results of this comparison are presented in Table 10. The table reveals that Taguchi yields two optimal outcomes when applied to two objectives, whereas PSO demonstrates its ability to produce a single optimal outcome that encompasses two distinct objectives. Specifically, the results indicate that Taguchi's optimal values of offset at 68 mm and cant angle at 50° generate responses that do not surpass the results obtained through PSO. Therefore, based on the findings presented in Table 10, it can be concluded that PSO outperforms Taguchi in optimizing RC aircraft parameters with dual objectives simultaneously.

Table 10. Comparison of Taguchi – PSO results

	Factor		Response	
	Offset (mm)	Cant Angle (°)	Cl/Cd_{max}	Cd_0
Taguchi	0	50	16.63645	0.018564
	68	50	16.622034	0.018768
PSO	0	50	16.63645	0.018564

4.0 CONCLUSION

In this study, the winglet design of an RC aeroplane was examined by varying offset and cant angle across four distinct levels. This study employed a combination of the Taguchi method for experimental design and the PSO algorithm for factor optimization. Performance metrics, including Cl/Cd_{max} and Cd_0, were calculated, and operational parameters were fine-tuned for optimization. The research findings indicate that when focused on maximizing Cl/Cd_{max}, the Taguchi method yielded results closely aligned with those obtained using the PSO algorithm. However, in the case of minimizing Cd_0, Taguchi exhibited less precision compared to the PSO algorithm. This discrepancy suggests that Taguchi is primarily adept at optimizing single objectives for the offset and cant angle factors. Conversely, the PSO algorithm offers an advantage in terms of efficiency by simultaneously optimizing multiple objectives, resulting in superior outcomes for this particular problem. Furthermore, it is worth noting that Taguchi's analysis ranks the offset as having a more significant influence on the drag coefficient. At the same time, the cant angle exerts a more pronounced effect on the lift-drag ratio coefficient.

XFLR5, as open-source and cost-effective software, is valuable for research in RC aeroplane design and offers significant benefits to aeromodelling clubs seeking to enhance their aircraft's performance. Additionally, for a deeper understanding of aerodynamic phenomena, complementary simulations such as CFD or small-scale wind tunnel testing can be employed to reinforce scientific knowledge and validate aerodynamic performance. This study contributed to understanding winglet design for RC aircraft and using the Taguchi method and PSO algorithm in this context.

5.0 REFERENCES

[1] P. Panagiotou and K. Yakinthos, "Aerodynamic efficiency and performance enhancement of fixed-wing UAVs," *Aerospace Science and Technology*, vol. 99, p. 105575, 2020.

[2] U.S. Department of Transportation, Aviation Maintenance Technician Handbook–Air frame, *Federal Aviation Administration*, FAA-H-8083-31B, Oklahoma City, OK, United States, 2023.

[3] S. Gudmundsson, General Aviation Aircraft Design: Applied Methods and Procedures. 1st Ed. *Butterworth-Heinemann*, United Kingdom, 2014.

[4] P. Panagiotou, P. Kaparos, and K. Yakinthos, "Winglet design and optimization for a MALE UAV using CFD," *Aerospace Science and Technology*, vol. 39, pp. 190–205, 2014.

[5] P. Panagiotou, S. Antoniou, and K. Yakinthos, "Cant angle morphing winglets investigation for the enhancement of the aerodynamic, stability and performance characteristics of a tactical Blended-Wing-Body UAV," *Aerospace Science and Technology*, vol. 123, p. 107467, 2022.

[6] R. T. Whitcomb, "A design approach and selected wind tunnel results at high subsonic speeds for wing-tip mounted winglets," *NASA Technical Note*, no. 19760019075, 1976.

[7] J. P. Eguea, P. D. Bravo-Mosquera, and F. M. Catalano, "Camber morphing winglet influence on aircraft drag breakdown and tip vortex structure," *Aerospace Science and Technology*, vol. 119, p. 107148, 2021.

[8] N. Sethi and S. Ahlawat, "Low-fidelity design optimization and development of a VTOL swarm UAV with an open-source framework," *Array*, vol. 14, p. 100183, 2022.

[9] M. El Adawy *et. al.*, "Design and fabrication of a fixed-wing Unmanned Aerial Vehicle (UAV)," *Ain Shams Engineering Journal*, vol. 14, no. 9, p. 102094, 2023.

[10] S. G. Kontogiannis, D. E. Mazarakos, and V. Kostopoulos, "ATLAS IV wing aerodynamic design: From conceptual approach to detailed optimization," *Aerospace Science and Technology*, vol. 56, pp. 135–147, 2016.

[11] P. Panagiotou, P. Kaparos, C. Salpingidou, and K. Yakinthos, "Aerodynamic design of a MALE UAV," *Aerospace Science and Technology*, vol. 50, pp. 127–138, 2016.

[12] J. Guerrero, M. Sanguineti, and K. Wittkowski, "CFD study of the impact of variable cant angle winglets on total drag reduction," *Aerospace*, vol. 5, no. 4, p. 126, 2018.

[13] S. Kapsalis, P. Panagiotou, and K. Yakinthos, "CFD-aided optimization of a tactical Blended-Wing-Body UAV platform using the Taguchi method," *Aerospace Science and Technology*, vol. 108, p. 106395, 2021.

[14] E. Atencio, F. Plaza-Muñoz, F. Muñoz-La Rivera, and J. A. Lozano-Galant, "Calibration of UAV flight parameters for pavement pothole detection using orthogonal arrays," *Automation in Construction*, vol. 143, p. 104545, 2022.

[15] A. Susanto, "Optimasi kinerja dan kestabilan unmanned aerial vehicle melalui pengaturan parameter dihedral dan tip-twist sayap dengan menerapkan metode artificial neural network-genetic algorithm," *Master Thesis*, Institut Teknologi Sepuluh Nopember Surabaya, 2021.

[16] F. Firdaus, "Optimasi kinerja dan kestabilan unmanned aerial vehicle melalui pengaturan parameter chord tip dan offset sayap dengan menerapkan metode artificial neural network-genetic algorithm," *Master Thesis*, Institut Teknologi Sepuluh Nopember Surabaya, 2021.

[17] F. D. Pertiwi, "Optimasi kinerja dan kestabilan unmanned aerial vehicle sebagai pengaruh konfigurasi blended winglet dengan menggunakan metode backpropagation neural network–genetic algorithm," *Master Thesis*, Institut Teknologi Sepuluh Nopember Surabaya, 2022.

[18] A. Boutemedjet, M. Samardžić, L. Rebhi, Z. Rajić, and T. Mouada, "UAV aerodynamic design involving genetic algorithm and artificial neural network for wing preliminary computation," *Aerospace Science and Technology*, vol. 84, pp. 464–483, 2019.

[19] R. Abnous, C. Zeng, S. Chowdhury, V. Maldonado, and P. Mancuso, "Conceptual design of a blended-wing-body tilt-arm hybrid unmanned aerial vehicle," in *58th AIAA/ASCE/AHS/ASC Structures, Structural Dynamics, and Materials Conference*, *Grapevine, Texas*, 2017, pp. 1-19.

[20] M. Baigang and W. Xiangyu, "A new aerodynamic optimization method with the consideration of dynamic stability," *International Journal of Aerospace Engineering*, vol. 2021, p. 5551094, 2021.

[21] T. Jiang and L. Jiang, "Optimization of UAV airfoil based on improved particle swarm optimization algorithm," *International Journal of Aerospace Engineering*, vol. 2022, p. 2828198, 2022.

[22] B. Mi, S. Cheng, Y. Luo, and H. Fan, "A new many-objective aerodynamic optimization method for symmetrical elliptic airfoils by PSO and direct-manipulation-based parametric mesh deformation," *Aerospace Science and Technology*, vol. 120, p. 107296, 2022.

[23] M. Bashir, S. Longtin-Martel, R. M. Botez, and T. Wong, "Aerodynamic design optimization of a morphing leading edge and trailing edge airfoil–Application on the UAS-S45," *Applied Sciences*, vol. 11, no. 4, 2021.

[24] M. Bashir, S. Longtin Martel, R. M. Botez, and T. Wong, "Aerodynamic design and performance optimization of camber adaptive winglet for the UAS-S45," in *AIAA SciTech 2022 Forum*, San Diego, California, United States, 2022.

[25] J. Tao, G. Sun, X. Wang, and L. Guo, "Robust optimization for a wing at drag divergence Mach number based on an improved PSO algorithm," *Aerospace Science and Technology*, vol. 92, pp. 653–667, 2019.

[26] M. Leahy, "Multidisciplinary design optimization of a morphing wingtip concept with multiple morphing stages at cruise," *Master Thesis*, University of Toronto, 2013.

[27] Z. Wei and S. Meijian, "Design optimization of aerodynamic shapes of a wing and its winglet using modified quantum-behaved particle swarm optimization algorithm," *Proceedings of the Institution of Mechanical Engineers, Part G: Journal of Aerospace Engineering*, vol. 228, no. 9, pp. 1638–1647, 2014.

[28] J. Tao, G. Sun, J. Si, and Z. Wang, "A robust design for a winglet based on NURBS-FFD method and PSO algorithm," *Aerospace Science and Technology*, vol. 70, pp. 568–577, 2017.

[29] N. K. Hieu and H. T. Loc, "Airfoil selection for fixed wing of small unmanned aerial vehicles," in *Recent Advances in Electrical Engineering and Related Sciences: Lecture Note in Electrical Engineering*, vol. 317, pp. 881–890, 2016.

[30] W. A. Widodo, "Studi numerik karakteristik aliran tiga dimensi pada body pesawat tanpa awak jenis cessna 182 menggunakan airfoil august 160 dan penambahan trapezoidal winglet variasi h/S= 0, 15; 0, 20; 0, 25 dengan cant angle 90˚," *Jurnal Teknik ITS*, vol. 9, no. 2, pp. B102–B107, 2021.

[31] F. D. Pertiwi and A. Wahjudi, "Numerical study of blended winglet geometry variations on unmanned aerial vehicle aerodynamic performance," *The International Journal of Mechanical Engineering and Sciences*, vol. 6, no. 1, pp. 31–36, 2022.

[32] I. H. Güzelbey, Y. Eraslan, and M. H. Doğru, "Numerical investigation of different airfoils at low Reynolds number in terms of aerodynamic performance of sailplanes by using XFLR5," *Karadeniz Fen Bilimleri Dergisi*, vol. 8, no. 1, pp. 47–65, 2018.

[33] A. Schumacher, E. Sjögren, and T. Persson, "Winglet effect on induced drag for a cessna 172 wing," *Bachelor Thesis*, KTH Flygteknik. 2014.

[34] A. Deperrois, "Part IV: Theoretical limitations and shortcomings of XLFR5," *XFLR5 Documentation,* vol. 1, pp. 1-33, 2019.

[35] I. Soejanto, Desain Eksperimen dengan Metode Taguchi, 1st Ed. *Yogyakarta: Graha Ilmu*, Indonesia, 2009.

[36] P. Woolf *et. al*., Chemical Process Dynamics and Controls, 1st Ed. *Chemical Process Dynamics and Controls*, *LibreTexts*, United States, p. 751, 2022.

[37] J. Kennedy and R. Eberhart, "Particle swarm optimization," in *Proceedings of ICNN'95 - International Conference on Neural Networks*, Perth, Australia, pp. 1942–1948, 1995.

[38] K. E. Parsopoulos and M. N. Vrahatis, Particle Awarm Optimization and Intelligence: Advances and Applications: Advances and Applications, 1st Ed. *IGI Global*, United States, 2010.

[39] C.-Y. Lee and M. Tuegeh, "An optimal solution for smooth and non-smooth cost functions-based economic dispatch problem," *Energies*, vol. 13, no. 14, p. 3721, 2020.